Journal of Saudi Chemical Society (2017) **21**, S445–S456

King Saud University

Journal of Saudi Chemical Society

www.ksu.edu.sa
www.sciencedirect.com

ORIGINAL ARTICLE

Synthesis of biologically active cadmium (II) complex with tridentate N_2O donor Schiff base: DFT study, binding mechanism of serum albumins (bovine, human) and fluorescent nanowires

Madhumita Hazra [a,b], **Tanushree Dolai** [b], **Subrata Giri** [c], **Animesh Patra** [b,*], **Subrata Kumar Dey** [a,*]

[a] *Department of Chemistry, Sidho-Kanho-Birsha University, Purulia 723101, India*
[b] *Postgraduate Department of Chemistry, Midnapore College, Midnapore 721101, India*
[c] *Department of Botany, Midnapore College, Midnapore 721101, India*

Received 5 July 2014; revised 17 October 2014; accepted 20 October 2014
Available online 21 November 2014

KEYWORDS

Cadmium complex;
Protein binding (BSA, HSA);
Optical properties;
SEM study;
Antibacterial and antioxidant activity

Abstract The photophysical properties of luminescent tetra-coordinated cadmium (II) complex formulated as [Cd(L)Cl],**HL** = (1-[(3-methyl-pyridine-2-ylimino)-methyl]-naphthalen-2-ol) were synthesized and characterized by analytical and spectroscopic methods. The density function theory calculations are used to investigate the electronic structures of the ligand and its complex. The interactions of cadmium (II) complex towards bovine serum albumin (BSA) and human serum albumin (HSA) were investigated using absorption and fluorescence spectroscopic techniques at pH 7.4. The quenching constants, binding constants and number of binding sites were determined by fluorescence quenching method. The calculated thermodynamic parameters (ΔG, ΔH, and ΔS) confirmed that the binding reaction is mainly entropy-driven and hydrophobic forces played an important role in the reaction. Here, we proposed a new synthetic procedure for the preparation of BSA and HSA with cadmium complex nanowires. The scanning electron microscopy images show that BSA and HSA with cadmium complex product are wire-like in structure. The complex shows enhanced antibacterial activity compared with the free ligand and standard antibiotic chloramphenicol. Antioxidant studies showed that the complex has significant antioxidant activity against DPPH.

* Corresponding authors.
E-mail addresses: animeshpatrarl@yahoo.com (A. Patra), skdjuchem@yahoo.com (S.K. Dey).
Peer review under responsibility of King Saud University.

Production and hosting by Elsevier

http://dx.doi.org/10.1016/j.jscs.2014.10.007

The obtained IC_{50} value of the DPPH activity for complex (IC_{50} = 138 μg/ml) showed excellent scavenging property compared to standard ascorbic acid.

1. Introduction

Transition metal complexes with Schiff-base ligand are important class of compounds in medicinal and pharmaceutical development because wide range of their applications, including antibacterial [1], antifungal [2] and anticancer properties [3]. Schiff bases are important intermediates in an enzymatic reactions involving interaction of the amino group of an enzyme, with a carbonyl group of the substrate. The Schiff bases have emerged as antimicrobial agents because of their broad spectrum of *in vitro* and *in vivo* chemotherapeutic activity.

Among biomacro molecules, the serum albumins are the major soluble protein constituent of the circulatory system and also transport protein [4]. The crystal structure of human serum albumin (HSA) revealed that the drug binding sites are located in sub-domains IIA and IIIA [5]. Bovine serum albumin (BSA) is structurally homologous to HSA [6]. Human serum albumin has one tryptophan (Trp-214) in sub-domain IIA, whereas BSA has two tryptophan moieties (Trp-134 and Trp-213) located in sub-domains IB and IIA, respectively. Albumins from blood plasma can bind with pyridoxal phosphate, Schiff-base ligands [7], and various metal complexes [8]. Therefore, the binding of drugs to serum albumin *in vitro*, considered as a model in protein chemistry to study the binding behaviour of proteins, research field in chemistry, life sciences and clinical medicine [9,10].

The design and synthesis of nanomaterials are important for nanotechnology and nanoscience. Adsorption of protein molecules on nanoparticles surface changes their biological systems [11]. These bioconjugate nanoparticles are important because of their potential applications in luminescence tagging, imaging, medical diagnostics. Protein conjugation nanoparticles have also been used as a strategy for increasing colloidal stability [12], conferring biochemical activity [13] and enhancing biocompatibility [14].

Our interest in nitrogen–oxygen polydentate chelators are addressed towards their potential applications [15] and we report an account of cadmium (II) complex with formula [Cd(L)Cl] **HL** = (1-[(3-methyl-pyridine-2-ylimino)-methyl]-naphthalen-2-ol). The BSA and HSA protein binding study of the cadmium (II) complex has been performed absorption and fluorescence spectroscopic study. The optical absorption and fluorescence emission property of the cadmium (II) complex was characterized and exhibited intense fluorescence emission. The antibacterial and antioxidant activity of the Schiff base and cadmium (II) complex demonstrate that the complex is higher activity than free ligand.

2. Experimental

2.1. Materials and physical measurements

All chemicals and reagents were obtained from commercial sources and used as received, unless otherwise stated. Solvents were distilled from an appropriate drying agent. The elemental (C, H, N) analyses were performed on a Perkin Elmer model 2400 elemental analyser. Cadmium analysis was carried out by Varian atomic absorption spectrophotometer (AAS) model-AA55B, GTA using graphite furnace. Electronic absorption spectra were recorded on a SHIMADZU UV-1800 spectrophotometer. The fluorescence spectra of EB bound to albumins were obtained in the Fluorimeter (Hitachi-2000) with thermostat. IR spectra (KBr discs, 4000–400 cm^{-1}) were recorded using a Perkin–Elmer FTIR model RX1 spectrometer. Molar conductances (M) were measured in a systronics conductivity metre 304 model using $\sim 10^{-3}$ mol L^{-1} solutions in DMF solvent. Electron spray ionization (ESI) mass spectra were recorded on a Qtof Micro YA263 mass spectrometer. ^{1}H NMR spectral data were recorded in suitable solvent using Bruker 300, 400, 500 MHz FT-NMR spectrometer and ^{13}C NMR was recorded in Bruker 400 MHz spectrometer using TMS as an internal standard in appropriate deuterated solvents. XRD was recorded in 'Rigaku Miniflex-II' X-ray diffractometer using CuKα radiation (λ = 0.154056 nm). The stock solutions of proteins (1.00×10^{-5} mol L^{-1}) were prepared by dissolving the solid HSA and BSA in 0.05 M phosphate buffer at pH 7.4 and stored at 0–4 °C in the dark. The concentrations of BSA and HSA were determined from optical density measurements, using the values of molar absorptivity of $\varepsilon 280$ = 44 720 and 35 700 M^{-1} cm^{-1} for BSA and HSA, respectively. Optical microscopy images were taken using an NIKON ECLIPSE LV100POL upright microscope equipped with a 12 V–50 W halogen lamp. The samples for optical microscopic study were prepared by placing a drop of colloidal solution onto a clean glass slide. Stock solution of complex was prepared in DMF because of the lower solubility in water. SEM study of nanoparticles was performed using Supra 40, Carl-ZEISS Pvt. Ltd Scanning Electron Microscope (SEM) with an accelerating voltage of 5 kV. Samples for the SEM study were prepared by drying a drop of the aqueous suspension of particles on a small glass slide followed by solvent evaporation under vacuum. To minimize sample charging, the dried samples were coated with a thin gold layer (< 5 nm) right before SEM study.

2.2. Preparation of the ligand (*HL*)

The ligand **HL** was prepared according to the literature procedure [15].

$C_{17}H_{14}N_2O$: Anal. Found: C, 77.86; H, 5.34; N, 10.68; Calc.: C, 77.12; H, 5.48; N, 10.24, m.p. 186 ± 1 °C; ESI-MS: $[M+H]^+$, *m/z*, 262.16; IR (KBr, cm^{-1}): $\nu_{O-H,}$ 3448, $\nu_{C=N,}$ 1472, $\nu_{CH=N,}$ 1623; ^{1}H NMR (δ, ppm in $CDCl_3 + CCl_4$): 15.686 (d, $1H_a$); 9.976 (d, $1H_b$); 8.30 (d, $1H_c$); 6.89 (d, $1H_d$); 8.15–7.04 (m, 9H); 2.498 (s, $1H_e$); ^{13}C NMR: 149.08 (C-9), 146.31 (C-1), 139.45 (C-7), 129.32–119.31 (Ar-C), 17.00 (C-6); Yield: 90%.

2.3. Preparation of [Cd(L)(Cl)]

To prepare this cadmium (II) complex a common procedure was followed as described below, using cadmium chloride and the organic ligand (**HL**) in equimolar ratio (1:1). A methanolic solution of **HL** (131 mg, 0.5 mmol) was mixed with (100 mg, 0.5 mmol) of cadmium chloride with stirring condition and the mixture was refluxed for 6 h. The orange colour cadmium (II) complex was collected by filtration and washing with methanol and cold water and then dried in vacuo. The pure crystallized product was obtained from methanol. Finally the product was verified by IR, ^{1}H NMR and mass spectroscopy.

[Cd(L)(Cl)]: $C_{17}H_{13}N_2CdOCl$: Anal. Found; C, 50.00; H, 3.18; N, 6.86; Cd, 27.45; Calc.: C, 49.84; H, 3.12; N, 6.84; Cd, 27.42. ESI MS (*m*/*z*): M^+ 408, $[M+2]^+$ 410. IR (cm^{-1}): $\nu_{CH=N}$, 1616; ν_{C-H}, 2943, $\nu_{C=N}$, 1469, ^{1}H NMR (δ, ppm in DMSO-d_6): 9.98 (d, $1H_b$); 8.38 (s, $1H_c$); 6.94 (s, $1H_d$); 8.19–7.20 (m, 9H); 2.52 (d, $1H_e$); m.p. 219 ± 1 °C; Λ_M (DMF): 12.16 $cm^2\ \Omega^{-1}\ M^{-1}$; Yield: 80%.

2.4. Synthesis of Cd-complex with BSA/HSA nanowires

The synthesis of Cd–BSA nanowires as described below, 8 μM BSA and 22 μM Cd(L)Cl are dissolved in 90 μL of phosphate buffer solution of pH 7.4. The mixture as allowed to incubate for 1 h at room temperature with continuous shaking. Incubation was followed with centrifuged at1100 rpm for about 30 min, which allows the removal of any unbound protein molecule and gives a dark orange solution of Cd–BSA nanowires (Scheme 1). In buffer solution (pH 7.4), negative ions of BSA molecules attached on the surface, which forms the attractive columbic interaction between the protein and the cadmium nanowires [16]. Similarly Cd–HSA nanowires were synthesized.

2.5. Theoretical methodology

All molecular calculations were performed in the gas phase using Density Functional Theory (DFT) using the B3LYP (Becke three-parameter Lee–Yang–Parr) exchange correlation functional [17]. The basis set LanL2DZ was used to cadmium (II) complex for all atoms. All calculations were carried out using the GAUSSIAN 09 program package with the aid of the Gauss View visualization program [18,19].

2.6. Protein (BSA and HSA) binding experiments

The quantitative analyses of the interaction between Cd (II) complex and serum albumins were performed by absorption spectra and fluorimetric titration in presence of phosphate buffer at pH 7.4. A 3.0 mL portion of aqueous solution of protein was titrated by addition of the appropriate concentration of Cd (II) complex solution (to give a final concentration of 4.5×10^{-6} mol L^{-1}). For every addition, the mixture solution was shaken and allowed to stand for 20 min, and then the fluorescence intensities were measured with an excitation wavelength of 280 nm.

2.7. Antimicrobial screening

The antibacterial activities of the ligand (**HL**) and its Cd (II) complex have been studied by agar disc diffusion method [20,21]. The antibacterial activities were done at 100 and 200 μg/mL concentrations of compound in DMF solvent by using three pathogenic gram negative bacteria (*Escherichia coli*, *Vibrio cholerae*, *Streptococcus pneumoniae*) and one gram positive pathogenic bacteria (*Bacillus cereus*). The solution of ligand and its Cd (II) complex was added to the agar plates. The DMF solvent was used as a negative control. Incubation of the plates was done at 37 °C for 24 h, inhibition of the

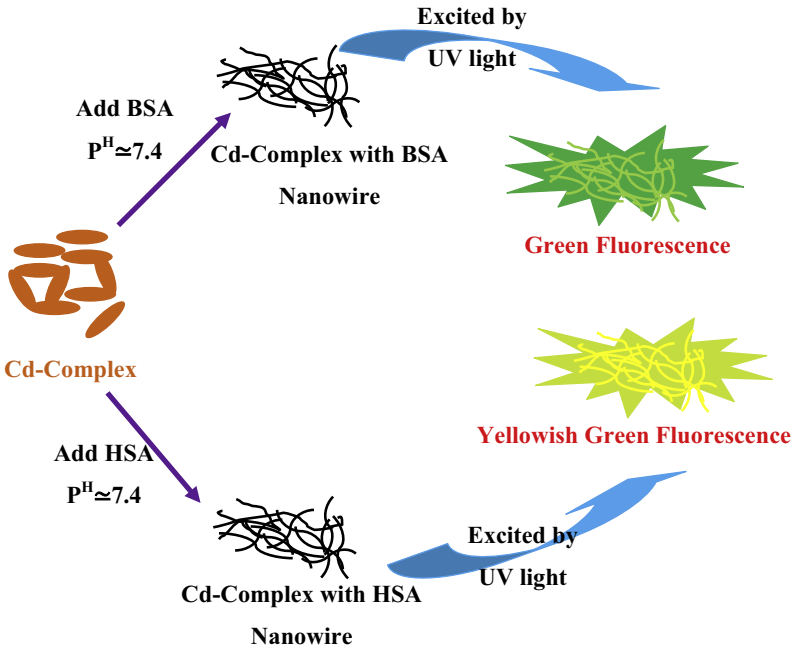

Scheme 1 A schematic representation for synthesis of Cd-complex with BSA or HSA nanowires.

organisms was measured and used to calculate mean of inhibition zones in millimetres.

2.8. DPPH radical scavenging activity

The free radical scavenging activity of the ligand and Cd (II) complex was determined by using 1,1-diphenyl-2-picrylhydrazyl (DPPH) free radical scavenging method. The compound was dissolved in hot methanol (20 mg/20 ml) and used as stock solution. From the stock solution, 1 mL of different concentrations (50–500 μg/mL) of sample in methanol were added to 4 mL of a 1.42×10^{-5} M DPPH solution and mixed, and then solution was left to stand at room temperature in the dark. After 30 min of incubation, the absorbance of the solution was measured at 520 nm using UV–Vis spectrophotometer [22,23]. Ascorbic acid used as standard, DPPH solution was used as control with-out the test compounds and methanol was used as blank. The percentage of scavenging activity of DPPH free radical was measured by using the following formula:

$$\% \text{ of scavenging activity} = \frac{[A_c - A_t]}{A_c} \times 100$$

where A_c is the absorbance of the control and A_t is the absorbance of sample. The scavenging activity was expressed as IC_{50} value which is defined as the concentration (μg/ml) of compound required for scavenging of DPPH radicals by 50%.

3. Results and discussion

3.1. Synthesis and characterization

The organic ligand (**HL** = (1-[(3-methyl-pyridine-2-ylimino)-methyl]-naphthalen-2-ol) was synthesized by the reaction of the respective of 3-methyl-2-amino pyridine (5.0 mmol) and then 5.0 mmol of 2-hydroxy-1-naphthaldehyde in presence of Ethanol. The complex was obtained in good yield from the equimolar reaction of the cadmium (II) chloride and **HL** in the methanol medium. The complex conductivity measurement in DMF solution results that the molar conductivity values of 12.16 $cm^2\ \Omega^{-1}\ M^{-1}$ suggest that complex exist in solution as a non-electrolyte. The complex is monomeric, non-hygroscopic, orange coloured solids, partly soluble in ethanol, methanol, and soluble in DMSO and DMF solvent. From Satisfactory analytical results such as conductivity, UV–Vis spectra and magnetic moment (μ = 0.0 B.M) indicate complex is distorted tetrahedral geometry.

3.2. Infrared, NMR, mass spectra and electronic spectral studies

The IR spectra provide valuable information regarding the nature of functional group attached to the metal atom. Infrared spectral data of the Schiff base showed several bands at 1472 and 1623 cm^{-1} due to Pyridine C=N and imine CH=N stretching vibrations in the solid state and a broad band in the region 3200–3432 cm^{-1} which attributed to the intramolecular hydrogen bonding. The hydroxyl hydrogen of ligand is replaced by a metal in complex and bands are shifted to lower frequency on complexation with cadmium (II) ion. New vibrations at 412 and 518 cm^{-1} which are not present in the free Schiff base are attributed to the existence of (Cd–O) and (Cd–N).

The ^{1}H NMR spectra of the cadmium (II) complex have been recorded in DMSO-d_6 (Fig. S1). The complex exhibits methyl proton (H_e) appeared at δ 2.52 ppm, aromatic pyridine proton (H_b) appeared at δ 9.98 ppm, H_c appeared at δ 8.38 ppm, H_d appeared at δ 6.94 ppm, aromatic and heteroaromatic proton signals at δ 8.19–7.20 ppm and DMSO-d_6 appeared at δ 3.45 ppm. Moreover, the weakening of the signal (H_a) at δ of ca. 15.68 attributable to –N–H...O proton in the spectra of the free Schiff base ligand; this signal is absent in the spectrum of its cadmium (II) complex. The result indicated that the Schiff base is coordinated to the metal ion in the enolic form by deprotonation. In the cadmium (II) complex, the aromatic and heteroaromatic proton signals appeared downfield, due to increased conjugation on coordination.

^{13}C NMR spectra of the complex (Fig. S2) and ligand showed analogous character. In a complex the hydroxyl carbon (C-1) was found at 150.04 ppm, pyridine carbon (C-2) at 147.74 ppm, imine carbon (C-3) at 141.35 ppm, and the methyl carbon (C-4) signal was found at 17.62 ppm and aromatic carbons at 120.5–130.6 ppm. The mass spectrum of the cadmium (II) complex also supports its projected formulation. The mass spectrum of complex was recorded (Fig. S3) and its indicates that the molecular ion peak m/z at 262.16, consistent with the molecular weight of the ligand, whereas its cadmium (II) complex shows the molecular ion peak at m/z 408.86, 262.16, 155, 107, 93 which confirms the stoichiometry of the cadmium (II) complex to be [Cd(L)Cl]. A weak peak at m/z 410.82 corresponds to $[M+2]^+$ peak possibly due to the presence of isotopic chlorine in the cadmium (II) complex.

The electronic spectrum of cadmium (II) complex was recorded in DMF at room temperature. All the spectra of complex shows lower bands than 400 nm are due to $\pi \rightarrow \pi^*$ and $n \rightarrow \pi^*$ transitions for the aromatic ring. An intense band at 255 nm is assigned to $\pi \rightarrow \pi^*$ transition along with the weak band at around 317 nm is due to a charge transfer $d(Cd) \rightarrow \pi^*$ transition (MLCT).

3.3. Powder diffraction studies

The X-ray powder pattern of cadmium (II) complex showing prominent peaks has been shown in Fig. 1. All the

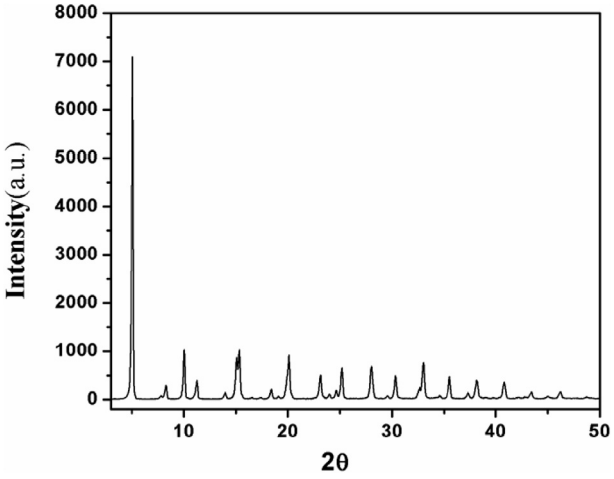

Figure 1 Powder XRD pattern of cadmium (II) complex.

prominent peaks of the different scale particles represent its crystalline nature. The powder patterns of different scale particles are well concurrent with each other and it indicates that different forms of complexes have the same structure and no impurities are detected from the XRD patterns [24].

3.4. Electronic structure

Full geometry optimization of **HL** and cadmium complex was carried out using density functional theory (DFT) at the B3LYP level in their ground state and the frontier orbitals of HOMO and LUMO of **HL** and complex are given in Fig. 2. From density functional theory (DFT) **HL** is not a planar structure, there occurs a conjugation between hydroxyl hydrogen and imine nitrogen atom. The selected bond distances and bond angles are reported in Table S1. Thus, it is apparent that HOMO of **HL**, the electrons are localized on pyridine and naphthalene ring but in complex electrons are largely localized in Cl-atom and imine group. In LUMO, electrons are largely localized on naphthalene ring. The HOMO–LUMO energy gap in the ground state of complex has been predicted to be 0.0336 eV and is not influenced on excitation. The N1—C1—N2 bond angle of **HL** is 119.30° but on complex formation the bond angle decreases about 99.90°. This indicate the organic moiety strongly bind to cadmium (II) ion. All the bond angles and bond length indicate the cadmium (II) complex is a distorted tetrahedral geometry.

3.5. Proteins (BSA and HSA) binding experiments

3.5.1. Absorption characteristics of BSA and HSA–Cd (II) complex

A pure BSA and HSA have a strong absorption band at 280 nm originating from the aromatic tryptophan and tyrosine residues. The absorption spectra of BSA and HSA in the absence and presence of Cd (II) complex was studied at different concentrations. From this study we observed that absorption of BSA and HSA increases regularly upon increasing the concentration of the complex [25], indicating the formation of a ground state complex. As dynamic quenching does not affect the absorption spectrum of quenching molecule and it only affects the exited states of quenching molecule, the observed changes in serum albumins absorbance in the presence of different concentrations of cadmium complex could be indicative of the occurrence of static quenching interaction between cadmium complex and serum albumins. The absorption spectra of Cd (II) complex with BSA and HSA are given in Fig. 3. From these data the apparent association constant (K_{app}) determined of the complex with BSA and HSA has been determined using the Benesi–Hildebrand equation [26]

$$1/(A_{obs} - A_0) = 1/(A_c - A_0) + 1/K_{app}(A_c - A_0)[comp]$$

where, A_{obs} is the observed absorbance of the solution containing different concentrations of the complex at 280 nm, A_0 and A_c are the absorbances of BSA, HSA and the complex at 280 nm, respectively, with a concentration of complex and K_{app} represents the apparent association constant. The

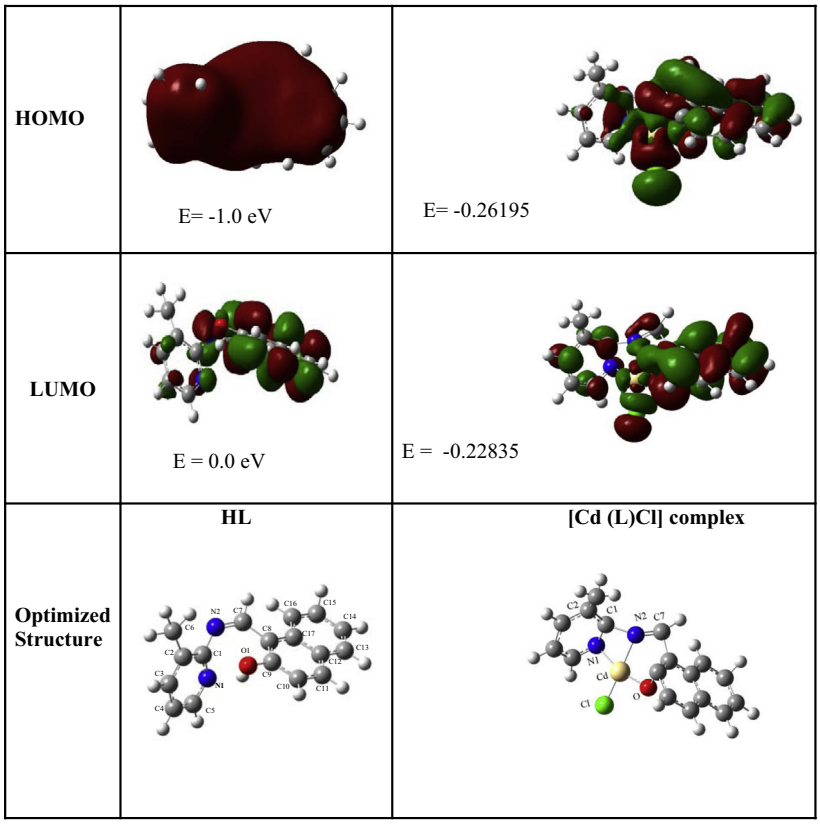

Figure 2 The **HOMO**, **LUMO** orbital's and optimized structures of **HL** and cadmium (II) complex obtained from DFT (B3LYP).

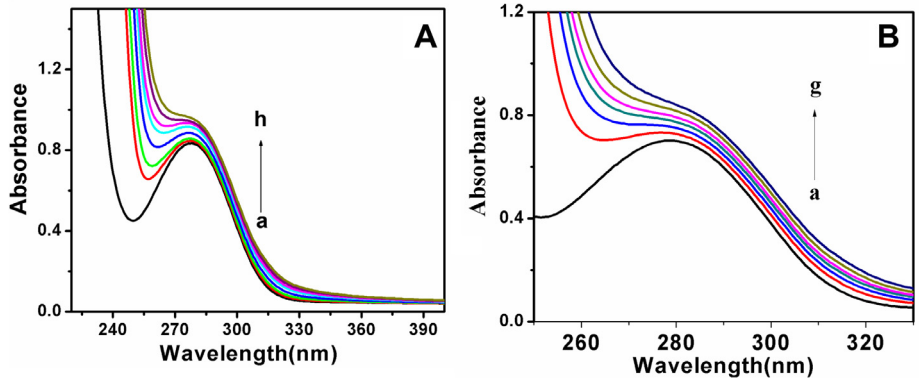

Figure 3 Electronic spectral titration of cadmium (II) complex with BSA (left, A) and HSA (right, B) at 280 nm in phosphate buffer. Arrow indicates the direction of change upon the increase concentration of BSA and HSA.

enhancement of absorbance at 280 nm was due to adsorption of the surface complex, based on the linear relationship between $1/(A_{obs} - A_0)$ *vs* reciprocal concentration of the complex with a slope equal to $1/K_{app}(A_c - A_0)$ and an intercept equal to $1/(A_c - A_0)$. The value of the apparent association constant (K_{app}) of BSA and HSA determined from this plot and the values were $3.62 \times 10^4\ M^{-1}$ and $3.16 \times 10^4\ M^{-1}$. All the plots represent a good linear relationship and cadmium (II) complex strongly adsorbed on the surface of BSA and HSA.

3.5.2. Fluorescence quenching of BSA and HSA by the cadmium complex

The interaction of Cd (II) complex with BSA and HSA was studying by the fluorescence emission spectrum with increasing the concentration of the cadmium complex. In presence of different concentrations of complex, the emission spectra of BSA and HSA was recorded in the wavelength range 300–500 nm by exciting the protein at 280 nm [27] and represented in Fig. 4. The result indicate that with increasing the concentration of the cadmium complex the fluorescence intensities of the proteins are regularly decreased. The fluorescence quenching is described by the Stern–Volmer relation [28]

$$F_0/F = 1 + K_{sv}[Q] = 1 + K_q\tau_0[Q]$$

where F_0 and F represent the fluorescence intensities in the absence and presence of quencher, respectively. K_{sv} is a linear Stern–Volmer quenching constant, Q is the concentration of quencher, k_q is the bimolecular quenching constant, and τ_0 is the average lifetime of protein in the absence of quencher, and its value is 10^{-8} s [29]. The corresponding Stern−Volmer quenching constants K_{SV} and quenching rate constants k_q are given in Table 1.The K_{sv} value calculated from the plot of F_0/F versus $[Q]$. All the Stern–Volmer plots represent (Fig. S4) a good linear relationship and indicating a strong affinity of the cadmium (II) complex to BSA and HSA.

Fluorescence quenching can be processed via different mechanisms, usually classified as dynamic quenching and static quenching. The Stern–Volmer plots represent a single quenching mechanism; either static or dynamic [30]. The dynamic and static quenching can be distinguished by differing in their dependence on temperature. In dynamic quenching, the quenching rate constant increases with increasing temperature and also indicates the faster diffusion but in the case of static quenching, the quenching rate constant decreases with increasing temperature. The K_{SV} increases with rising temperature given in Table 1, indicating that the fluorescence quenching of proteins by the Cd (II) complex is a dynamic quenching mechanism. The obtained k_q values in Table 1 for the compound is on the order of $10^{13}\ L\ mol^{-1}\ s^{-1}$, which is 1000-fold higher than the maximum value possible for diffusion controlled quenching (i.e., $2.0 \times 10^{10}\ L\ mol^{-1}\ s^{-1}$) [31]. This observation suggests that there is a specific interaction between serum albumins and cadmium complex. Again the Stern–Volmer quenching constant K_{SV} at different temperatures (300 and 310 K) is directly related with temperature so the probable quenching mechanism may be dynamic rather than static.

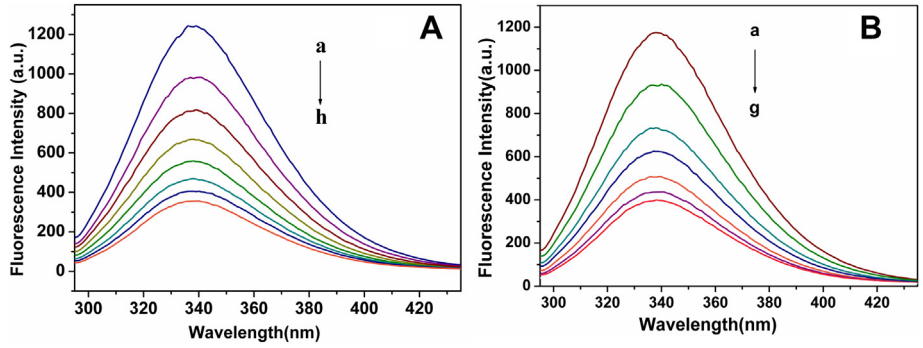

Figure 4 Change in fluorescence spectra of BSA (left, A) and HSA (right, B) through their titration with cadmium (II) complex in phosphate buffer. The concentration of complex varied from 0.0 to $4.5 \times 10^{-6}\ M\ L^{-1}$; λ_{ex} = 280 nm and pH 7.4.

Table 1 The quenching constants of BSA/HSA by cadmium (II) complex.

Complex	T (K)	K_{sv} (L Mol^{-1})	K_q (L Mol^{-1} S^{-1})
Cd–BSA	300	6.94×10^4	6.94×10^{13}
	310	7.18×10^4	7.18×10^{13}
Cd–HSA	300	4.92×10^4	4.92×10^{13}
	310	5.11×10^4	5.11×10^{13}

UV–Vis absorption measurements are used to study structural changes and complex formation. For a dynamic quenching, the absorption spectra of the substance is not changed, and fluorescence molecule is influenced by quenchers at the excited state, but for static quenching, a new compound is formed between the ground state of the fluorescent substance and quencher therefore, the absorption spectra of fluorescence substance would be considerably influenced. The absorption spectra of BSA and HSA in the absence and presence of Cd (II) complex was studied at the same concentrations (2.5×10^{-6} mol L^{-1}). The UV absorption spectrum of both proteins shows a weak band with a maximum at 280 nm (Fig. 5). The absorption intensity of the 280 nm peaks is increased by addition of Cd (II) complex, indicating that more aromatic acid residues were extended into the aqueous environment. This result indicated that the microenvironment of the three aromatic acid residues was altered and the tertiary structure of HSA and BSA was destroyed. These results show that the interaction between Cd (II) complex and proteins (HSA and BSA) was mainly a static quenching mechanism.

The calculation of K_{SV} from Stern–Volmer plots demonstrates that varying temperature has a moderate effect on the fluorescence quenching by Cd (II) complex. Therefore the quenching data were analysed according to the modified Stern–Volmer equation [32]

$$\frac{F_0}{F_0 - F} = \frac{1}{f_a K_a}\frac{1}{[Q]} + \frac{1}{f_a}$$

where, K_a is the effective quenching constant for the accessible fluorophores, and f_a is the fraction of accessible fluorescence. The plots of $F_0/F_0 - F$ versus $1/[Q]$ show a good linear relationship (Fig. 6), and corresponding K_a values at different temperatures are given in Table 2. The results show that the binding constants between Cd (II) complex and proteins are quite high. Stern–Volmer plots and modified Stern–Volmer plots for the quenching of by Cd (II) complex at different temperatures are compared. All the result indicates that Ka and K_{SV}'s constants increases with increasing temperature.

3.6. Analysis of binding site

Number of binding sites can be calculated from fluorescence titration data using the following equation [33]

$$\log\,[(F_0 - F)/F] = \log\,K_b + n \log\,[Q]$$

K_b and n is the binding constant and binding site of Cd (II) complex. According to the experimental results, the linear fitting plots of log $[(F_0 - F)/F]$ versus log$[Q]$ can be observed (Fig. 7). The corresponding K_b and n values, evaluated from the slopes and intercepts of the linear plots, respectively, are summarized in Table 3. As seen, the value of n is nearly 1 for binding of cadmium complex to the proteins used, which indicates that proteins bind to complex 1:1 M ratio.

3.7. Thermodynamic parameters and mode of binding

In general, small molecule bound to biomacromolecule through hydrogen bonding, Van der Waal force, electrostatic and hydrophobic interactions. The Thermodynamic parameters free energy (ΔG), enthalpy change (ΔH) and entropy change (ΔS) are important for the study of binding modes. The Thermodynamic parameters for a binding reaction can be calculated from the following van't Hoff equation:

$$\ln\frac{K_2}{K_1} = \left(\frac{1}{T_1} - \frac{1}{T_2}\right)\frac{\Delta H}{R} \text{ and } \Delta G = \Delta H - T\Delta S$$

where K is the equilibrium binding constant at the corresponding temperature, K_1 and K_2 are the binding constant at temperature T_1 and T_2 and R is the gas constant. The Thermodynamic parameters for the system of serum albumins cadmium complex are given in Table 2. According to Ross and Subramanian [34] have used the sign and magnitude of the thermodynamic parameters to decide various kinds of

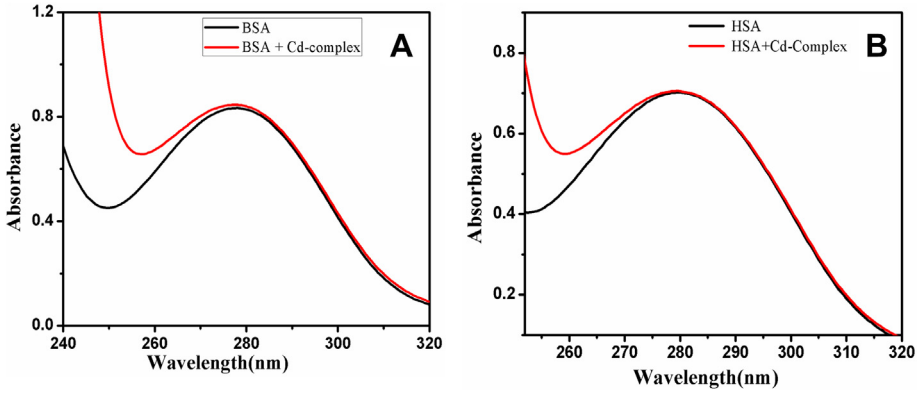

Figure 5 The UV–Vis absorption spectra of BSA (left, A) and HSA (right, B) in the absence and presence of cadmium (II) complex. Black line: the absorption spectrum of proteins. Red line: the absorption spectrum of proteins in the presence of cadmium (II) complex at the same concentration, c(BSA) c(HSA) = c(cadmium (II) complex) = 2.5×10^{-6} mol L^{-1}.

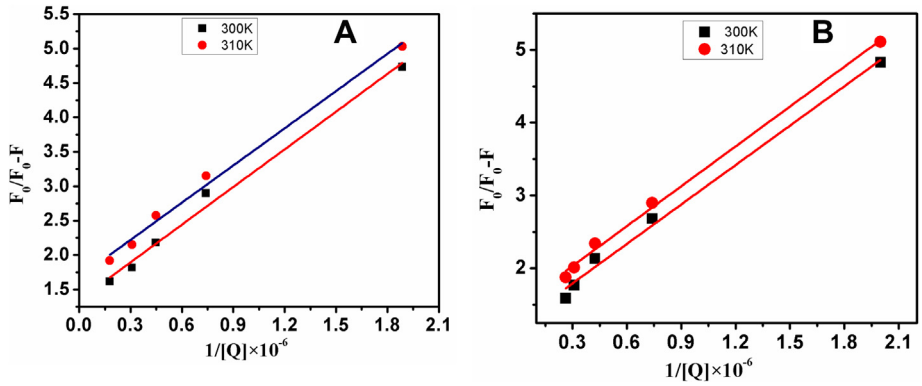

Figure 6 Plot of $F_0/F_0 - F$ against [Q] in case of fluorescence quenching of BSA (left, A) and HSA (right, B) through their titration with cadmium (II) complex in phosphate buffer at 300 K (■) and 310 K (●).

Table 2 Apparent binding constant and thermodynamic parameters for the interaction of cadmium (II) complex with BSA/HSA at different temperatures.

Complex	T (K)	K_a (L Mol^{-1})	n	ΔH (kJ Mol^{-1})	ΔG (kJ Mol^{-1})	ΔS (J Mol^{-1} K^{-1})
Cd–BSA	300	1.64×10^4	1.01	36.524	−24.206	202.4
	310	2.17×10^4	1.04		−25.734	200.8
Cd–HSA	300	1.48×10^4	1.02	32.731	−23.950	188.9
	310	2.26×10^4	1.02		−25.839	188.93

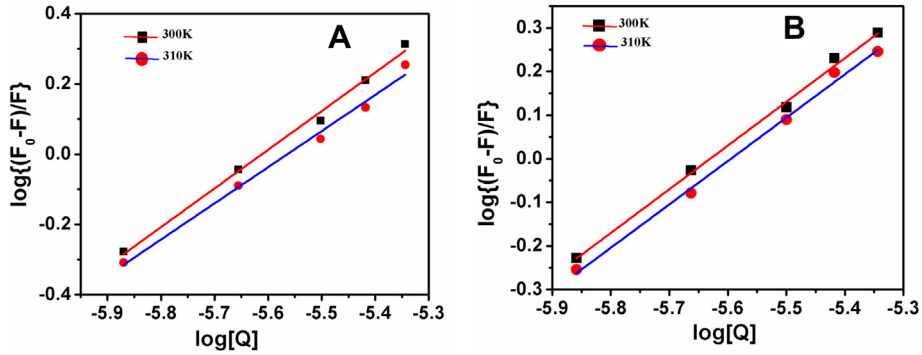

Figure 7 Double-log plots of cadmium (II) complex quenching effect on BSA (left, A) and HSA (right, B) fluorescence at 300 K (■) and 310 K (●).

Table 3 The binding constants and the number of binding sites of cadmium (II) compound with BSA and HSA at different temperature.

Complex	T (K)	K_b (L Mol^{-1})	n
Cd–BSA	300	4.58×10^4	0.92
	310	5.62×10^4	0.92
Cd–HSA	300	1.81×10^4	0.91
	310	2.25×10^4	0.92

interactions that may take place in protein association processes. From the point of view a positive ΔS and ΔH value is evidence for hydrophobic interactions, while those with $\Delta H < 0$ and $\Delta S < 0$ by hydrogen-bonding or Van der Waals interactions. The positive value of ΔH and ΔS indicates the major contribution in complexation is hydrophobic interaction and that the interaction is entropy driven process [35]. In addition to hydrophobic interaction, a possible covalent bonding may be also considered. For a covalent bond formation ΔH expected should be $\geqslant 120$ kJ mol^{-1}, however, the value of ΔH obtained here (about 36 and 32 kJ mol^{-1} for BSA and HSA, respectively) so it cannot expected for a covalent bond formation. In addition, we found that these complexes remain neutral tetra-coordinated and there is no empty position for coordination on Cd (II) to form covalent bond with albumins. Moreover, a larger contribution of a positive ΔS value, indicating that the main interaction was hydrophobic contact between complex and albumins. Hence increase the temperature hydrophobic interaction is increases, and this result indicates the increasing character of binding sites therefore a very stable complex is formed with high K_b value.

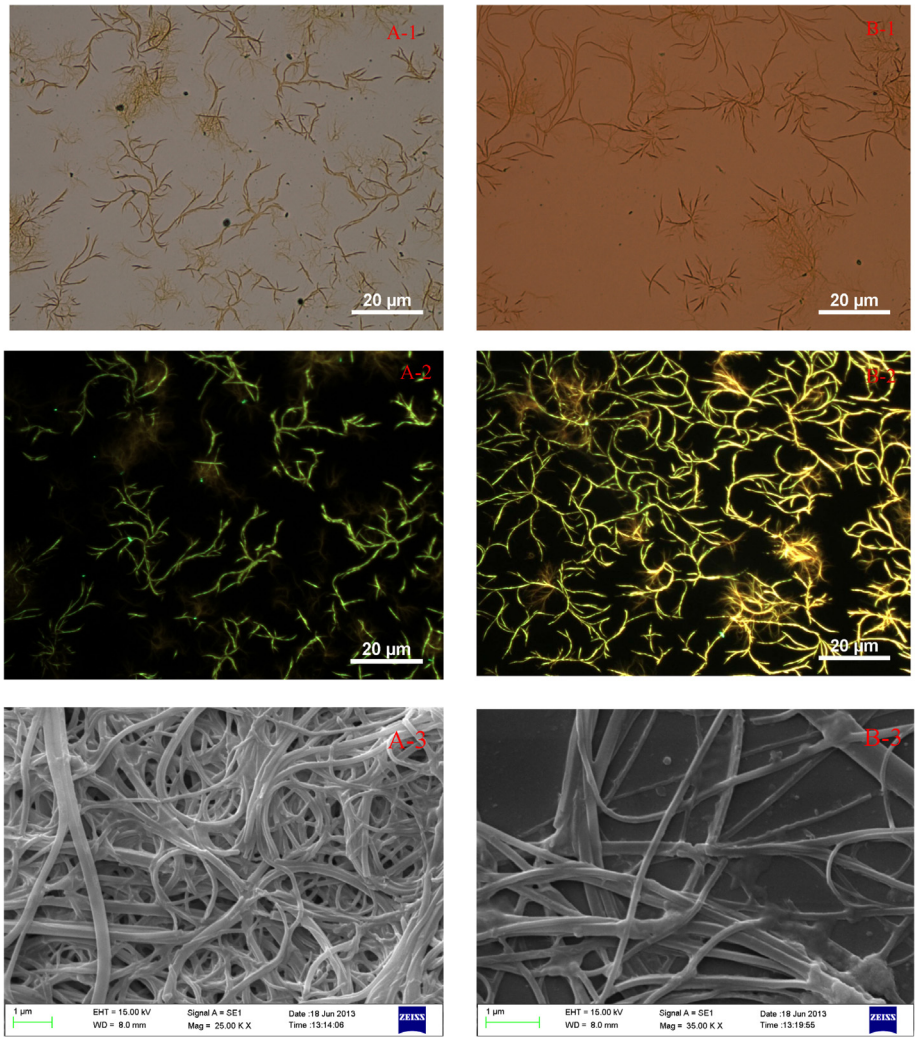

Figure 8 Optical, fluorescence microscopy and SEM image of cadmium (II) complex with BSA (A-1, A-2, A-3) and HSA (B-1, B-2, B-3) nanowires, respectively.

3.8. SEM and fluorescence microscopy study for crystallization of Cd-complex with BSA and HSA

The intense luminescence property of cadmium (II) complex with BSA and HSA suggests that optical and fluorescence microscopy will be a useful tool to investigate the morphology of the nanostructures (Fig. 8). Optical micrograph of sample-A and sample-B shows formation of wire shaped cadmium (II) complex with BSA and HSA, respectively. Upon excitation with blue light sample-A shows green luminescence and sample-B shows yellowish green luminescence. This suggests that the cadmium (II) complex molecules have been incorporated into the BSA or HSA microparticles during the solution-based route process and they are likely to be distributed randomly. It is supposed that during the formation of the doped microparticles, hydrophobic and π–π interactions induce the aggregation of BSA or HSA and cadmium (II) complex molecules into wires [36].

Scanning electron microscopy (SEM) has been routinely applied as an effective tool for the characterization of surface morphology of cadmium (II) complex loaded BSA and HSA. The SEM images [Fig. 8(A-3 and B-3)] demonstrate that the final products consist of a large quantity of nanowires in both case with a average diameter of about 102 nm and a typical length of several tens of micrometers. These images demonstrate the nanowires could be easily produced in large-scale using the present method. Some nanowires grow together with each other due to physical adsorption on the surface of the wires.

3.9. Antibacterial activity

Antibacterial activity of the ligand and its cadmium (II) complex are given in Fig. 9. Comparison the biological activity of the synthesized ligand and its cadmium (II) compound with standard antibiotic chloramphenicol. From the antibacterial studies it is inferred that, complex has higher activity than ligand. The hight of the bar represent the activity of ligand and complexes with respect to standard chloramphenicol antibiotic. The increased activity of the metal chelates can be explained by overtone concept and the Tweedy chelation theory. The variation in the activity of complex against some dif-

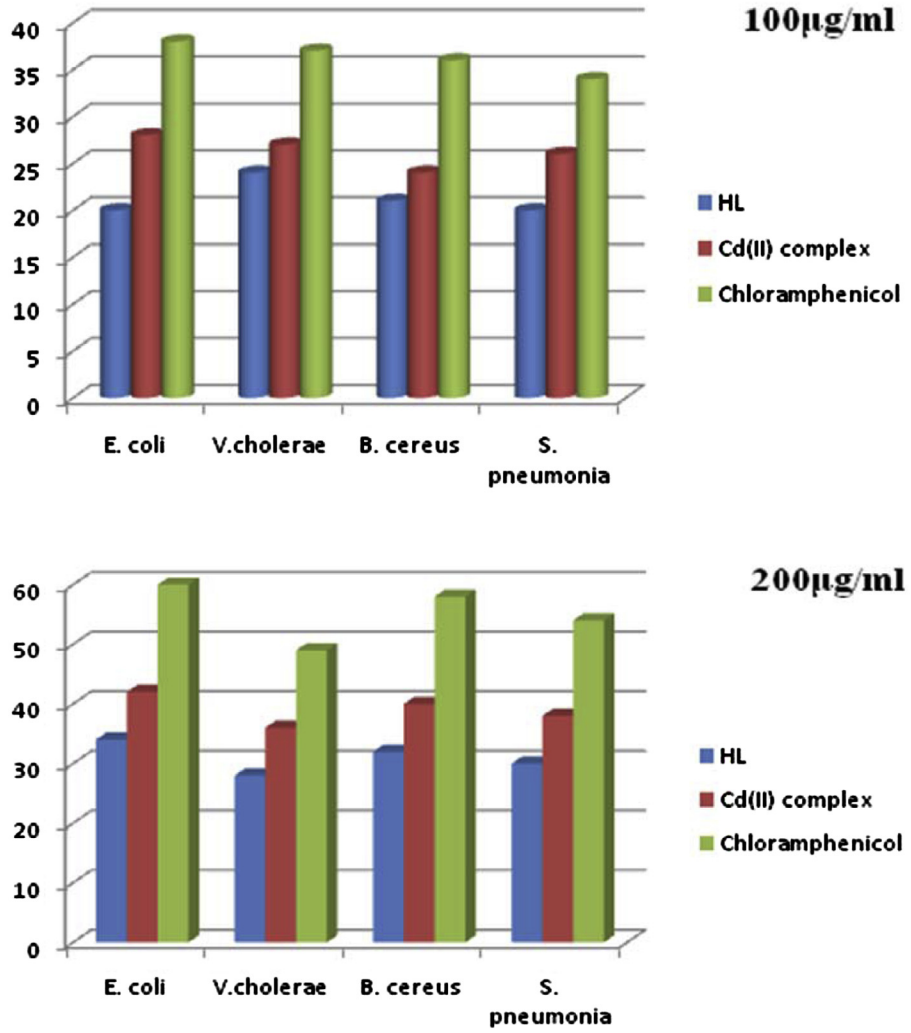

Figure 9 Antibacterial activity of ligand and its cadmium (II) complex were done at 100 and 200 µg/mL concentrations.

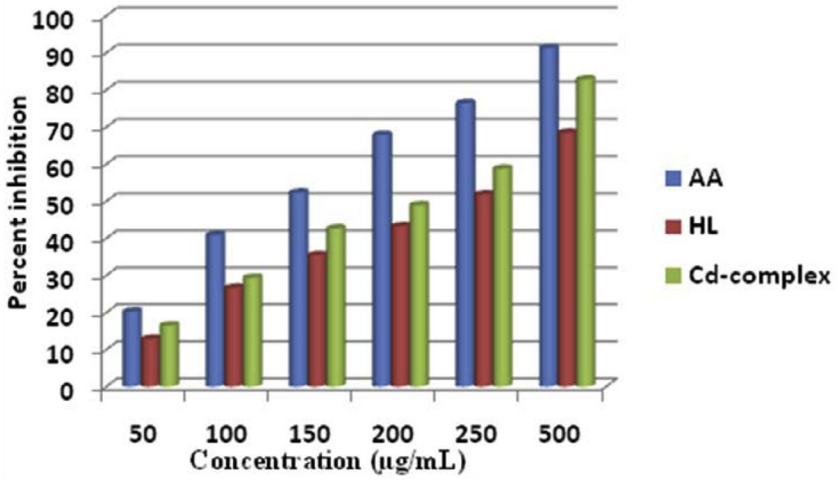

Figure 10 Comparison the antioxidant activity of Ligand (**HL**), cadmium (II) complex and standard ascorbic acid.

ferent organisms depend either on the impermeability of the cells of the microbes or difference in ribosome of microbial cells [37,38]. Enhancement of activity of the compound is due to the presence of hydroxy and methyl groups in title compounds. In a complex, increases the delocalization of π-electrons over the whole chelate ring and increase the lipophilic

Table 4 IC_{50} values of test compounds (μg/ml).

Compounds	AA	**HL**	Cd-complex
IC_{50} value (μg/ml)	130	165	138

character of the metal complex. This increased lipophilicity also helps the penetration of the bacterial cell membranes and blocks the metal binding sites in enzymes of microorganisms and restricts further growth of the microorganisms.

3.10. Antioxidant activity

The result of free radical scavenging activity of methanolic solutions of ligand and its compound at different concentrations are shown in Fig. 10. From results it is evident that free radical scavenging activity of the compound was concentration dependent. The complex possessed stronger antioxidant activity than their corresponding ligand [39,40]. It can be concluded that a less scavenging activity of ligand when compared to that of complexes which is due to the chelation of ligand with the central metal atom, as a result the presence of electron releasing hydroxyl and electron donating methyl group in ligand moiety able prominent improvement in radical scavenging activity. Ascorbic acid, used as a standard, showed stronger antioxidant activity than that of synthesized compound. The cadmium (II) complex showed strong ability with DPPH and expressed an IC_{50} value of 138.0 μg/ml lower than that of standard ascorbic acid (130.0 μg/ml), indicating they possessed stronger antioxidant activity than corresponding ligand **HL** (IC_{50} value of ligand is 165.0 μg/ml). The comparative antioxidant activity of ligand, cadmium (II) compound and ascorbic acid as a standard is shown in Table 4.

4. Conclusions

The synthesized cadmium (II) complex was characterized by using spectral and elemental analysis. The ^{1}H NMR and DFT calculation in support of the distorted tetrahedral configuration of cadmium (II) complex. From spectroscopic methods values Cd (II) complex strongly bind with BSA and HSA through a static quenching mechanism. Also Stern–Volmer constant indicate that the fluorescence quenching proceeds through a static process. The thermodynamic parameters (ΔG, ΔH, and ΔS) suggest that hydrophobic forces played a major role in the binding reaction and the process is endothermic. The optical absorption and fluorescence emission properties of the nanowires were characterized and exhibited intense fluorescence emission. The obtained cadmium (II) complex with BSA and HSA nanowires could be introduced as the building block for novel optoelectronic devices. The scanning electron microscopy images show that BSA and HSA with cadmium complex produce wire-like in structure. The antibacterial screening results cadmium (II) complex exhibited remarkable antimicrobial potency. Moreover, the complex exhibited stronger antioxidant effects than corresponding ligand and good candidates for use in a variety of applications. The biological significance of this work is evident since albumin serves as an endogenous carrier for the complex in the body, which could be a useful guide for further drug design.

Acknowledgment

We are thankful to Prof. Pabitra Chattopadhyay, Dept. of Chemistry, Burdwan University, Burdwan, for his moral support, encouragement and guidance.

Appendix A. Supplementary data

Supplementary data associated with this article can be found, in the online version, at http://dx.doi.org/10.1016/j.jscs.2014.10.007.

References

[1] S.H. Etaiw, D.M.A. El-Aziz, E.H. Abd El-Zaher, E.A. Ali, Synthesis, spectral, antimicrobial and antitumor assessment of Schiff base derived from 2-aminobenzothiazole and its transition metal complexes, Spectrochim. Acta Part A Mol. Biomol. Spectrosc. 79 (2011) 1331–1337.
[2] P. Panneerselvam, R.B. Nair, G. Vijayalakshmi, E.H. Subramanian, S.K. Sridhar, Synthesis of Schiff bases of 4-(4-aminophenyl)-morpholine as potential antimicrobial agents, Eur. J. Med. Chem. 40 (2005) 225–229.
[3] M. Ganeshpandian, R. Loganathan, E. Suresh, A. Riyasdeen, M.A. Akbarshad, M. Palaniandavar, New ruthenium (II) arene complexes of anthracenyl-appended diazacycloalkanes: effect of ligand intercalation and hydrophobicity on DNA and protein binding and cleavage and cytotoxicity, Dalton Trans. 43 (2014) 1203–1219.
[4] S. Soares, N. Mateus, V.D. Freitas, Interaction of different polyphenols with bovine serum albumin (BSA) and human salivary alpha-amylase (HSA) by fluorescence quenching, J. Agric. Food Chem. 55 (2007) 6726–6735.
[5] A. Sulkowska, Interaction of drugs with bovine and human serum albumin, J. Mol. Struct. 614 (2002) 227–232.
[6] K. Hirayama, S. Akashi, M. Furuya, K. Fukuhara, Rapid confirmation and revision of the primary structure of bovine serum albumin by ESIMS and Frit-FAB LC/MS, Biochim. Biophys. Res. Commun. 173 (1990) 639–646.
[7] P. Roy, M. Manassero, Tetranuclear copper(II)–Schiff-base complexes as active catalysts for oxidation of cyclohexane and toluene, Dalton Trans. 39 (2010) 1539–1545.
[8] G.B. Bagihalli, P.G. Avaji, S.A. Patil, P.S. Badami, Synthesis, spectral characterization, in vitro antibacterial, antifungal and cytotoxic activities of Co(II), Ni(II) and Cu(II) complexes with 1,2,4-triazole Schiff bases, Eur. J. Med. Chem. 43 (2008) 2639–2649.
[9] B. Bharti, J. Meissner, S.H.L. Klapp, G.H. Findenegg, Bridging interactions of proteins with silica nanoparticles: the influence of pH, ionic strength and protein concentration, Soft Matter 10 (2014) 718–728.
[10] F. Yu, V.M. Cangelosi, M.L. Zastrow, M. Tegoni, J.S. Plegaria, A.G. Tebo, C.S. Mocny, L. Ruckthong, H. Qayyum, V.L. Pecoraro, Protein design: toward functional metallo enzymes, Chem. Rev. 114 (2014) 3495–3578.
[11] D.C. Carter, X.J. Ho, Structure of serum albumin, Adv. Protein Chem. 45 (1994) 153–203.
[12] T. Yang, Z. Li, L. Wang, C. Guo, Y. Sun, Synthesis, characterization, and self-assembly of protein lysozyme monolayer-stabilized gold nanoparticles, Langmuir 23 (2007) 10533–10538.
[13] G. Mandal, M. Bardhan, T. Ganguly, Occurrence of Forster resonance energy transfer between quantum dots and gold nanoparticles in the presence of a biomolecule, J. Phys. Chem. C 115 (2011) 20840–20848.

[14] H. Mattoussi, J.M. Mauro, E.R. Goldman, G.P. Anderson, V.C. Sundar, F.B. Mikulec, M.G. Bawendi, Self-assembly of CdSe-ZnS quantum dot bioconjugates using an engineered recombinant protein, J. Am. Chem. Soc. 122 (2000) 12142–12150.
[15] M. Hazra, T. Dolai, A. Pandey, S.K. Dey, A. Patra, Fluorescent copper(II) complexes: the electron transfer mechanism, interaction with bovine serum albumin (BSA) and antibacterial activity, J. Saudi Chem. Soc. 21 (2017) S240–S247.
[16] L. Liu, H.Z. Zheng, Z.J. Zhang, Y.M. Huang, S.M. Chen, Y.F. Hu, Photoluminescence from water-soluble BSA-protected gold nanoparticles, Spectrochim. Acta Part A Mol. Biomol. Spectrosc. 69 (2008) 701–705.
[17] C. Lee, W. Yang, R.G. Parr, Development of the Colle-Salvetti correlation-energy formula into a functional of the electron density, Phys. Rev. B 37 (1988) 785–789.
[18] A.D. Becke, Density-functional exchange-energy approximation with correct asymptotic behavior, Phys. Rev. A 38 (1988) 3098–3100.
[19] S. Roy, T.K. Mondal, P. Mitra, E.L. Torres, C. Sinha, Synthesis, structure, spectroscopic properties, electrochemistry, and DFT correlative studies of N-[(2-pyridyl)methyliden]-6-coumarin complexes of Cu(I) and Ag(I), Polyhedron 30 (2011) 913–922.
[20] R.A. Sheikh, S. Shreaz, G.S. Sharma, L.A. Khan, A.A. Hashmi, Synthesis, characterization and antimicrobial screening of a novel organylborate ligand, potassium hydro(phthalyl)(salicylyl)borate and its Co(II), Ni(II), and Cu(II) complexes, J. Saudi Chem. Soc. 16 (2012) 353–361.
[21] C.R. Prakash, S. Raja, Synthesis, characterization and in vitro antimicrobial activity of some novel 5-substituted Schiff and Mannich base of isatin derivatives, J. Saudi Chem. Soc. 17 (2013) 337–344.
[22] E. Apostolidis, Y.I. Kwon, K. Shetty, Inhibitory potential of herb, fruit, and fungal-enriched cheese against key enzymes linked to type 2 diabetes and hypertension, Innov. Food Sci. Emerg. Technol. 8 (2007) 46–54.
[23] I. Correia, A. Nunes, I.F. Duarte, A. Barros, I. Delgadillo, Sorghum fermentation followed by spectroscopic techniques, Food Chem. 90 (2014) 853–859.
[24] M. Hazra, T. Dolai, A. Pandey, S.K. Dey, A. Patra, Synthesis and characterization of four coordinated palladium (II) complex with N2O donor Schiff base: interaction with calf thymus-DNA, density functional theory study and antibacterial activity, J. Chem. Biol. Interfaces 1 (2013) 100–107.
[25] A. Patra, B. Sen, S. Sarkar, A. Pandey, E. Zangrando, P. Chattopadhyay, Nickel(II) complexes with 2-(pyridin-3-ylmethylsulfanyl)phenylamine and halide/pseudohalides: synthesis, structural characterisation, interaction with CT-DNA and bovine serum albumin, and antibacterial activity, Polyhedron 51 (2013) 156–163.
[26] H.A. Benesi, J.H. Hildebrand, A spectrophotometric investigation of the interaction of iodine with aromatic hydrocarbons, J. Am. Chem. Soc. 71 (1949) 2703–2707.
[27] S. Sarkar, B. Das, Synthesis and characterization of mononuclear copper (II) complex of tetradentate N2S2 donor set and the study of DNA and bovine serum albumin binding, Complex Met. 1 (2014) 80–87.
[28] O. Stern, M. Volmer, On the quenching-time of fluorescence, Z. Phys. 20 (1919) 183–188.
[29] F. Samari, B. Hemmateenejad, M. Shamsipur, M. Rashidi, H. Samouei, Affinity of two novel five-coordinated anticancer Pt(II) complexes to human and bovine serum albumins: a spectroscopic approach, Inorg. Chem. 51 (2012) 3454–3464.
[30] W. He, Y. Li, C. Xue, Z. Hu, X. Chen, F. Sheng, Effect of Chinese medicine alpinetin on the structure of human serum albumin, Bioorg. Med. Chem. 13 (2005) 1837–1845.
[31] X. Zhao, R. Liu, Z. Chi, Y. Teng, P. Qin, New insights into the behavior of bovine serum albumin adsorbed onto carbon nanotubes: comprehensive spectroscopic studies, J. Phys. Chem. B 114 (2010) 5625–5631.
[32] T. Okajima, Y. Kawata, K. Hamaguchi, Chemical modification of tryptophan residues and stability changes in proteins, Biochemistry 29 (1990) 9168–9175.
[33] A. Kathiravan, R. Renganathan, Photoinduced interactions between colloidal TiO2 nanoparticles and calf thymus-DNA, Polyhedron 28 (2009) 1374–1378.
[34] P.D. Ross, S. Subramanian, Thermodynamics of protein association reactions: forces contributing to stability, Biochemistry 20 (1981) 3096–3102.
[35] G. Mandal, M. Bardhan, T. Ganguly, Interaction of bovine serum albumin and albumin-gold nanoconjugates with l-aspartic acid. A spectroscopic approach, Colloids Surf., B: Biointerfaces 81 (2010) 178–184.
[36] W. Chen, Q. Peng, Y. Li, Luminescent bis-(8-hydroxyquinoline) cadmium complex nanorods, Cryst. Growth Des. 8 (2008) 564–567.
[37] J. Joseph, K. Nagashri, G.A. Bibin Rani, Synthesis, characterization and antimicrobial activities of copper complexes derived from 4-aminoantipyrine derivatives, J. Saudi Chem. Soc. 17 (2013) 285–294.
[38] N. Raman, A. Kulandaisamy, A. Shunmugasundaram, K. Jeyasubramanian, Synthesis, spectral, redox and antimicrobial activities of Schiff base complexes derived from 1-phenyl-2,3-dimethyl-4-aminopyrazol-5-one and acetoacetanilide, Trans. Met. Chem. 26 (2001) 131–135.
[39] A.B. Shori, A.S. Baba, Antioxidant activity and inhibition of key enzymes linked to type-2 diabetes and hypertension by *Azadirachta indica*-yogurt, J. Saudi Chem. Soc. 17 (2013) 295–301.
[40] P. Sithisarn, R. Supabphol, W. Gritsanapan, Antioxidant activity of Siamese neem tree (VP1209), J. Ethnopharmacol. 99 (2005) 109–112.